References

[1]Koide, S., Griesel, C. J. W., and Stollery, J. L., "Correlation of Shock Angles Caused by Rhombic Delta Wings," *AIAA Journal* (to be published).

[2]Deng, X., Liao, L., and Zhang, H., "Improvement of Conical Similarity Rules in Swept Shock Wave/Boundary Layer Interaction," AIAA Paper 93-2941, July 1993.

[3]Fomison, N. R., and Stollery, J. L., "The Effects of Sweep and Bluntness on a Glancing Shock Wave Turbulent Boundary Layer Interaction," AGARD CP 428, April 1987.

[4]Settles, G. S., and Lu, F. K., "Conical Similarity of Shock/Boundary-Layer Interactions Generated by Swept and Unswept Fins," *AIAA Journal*, Vol. 23, No. 7, 1985, pp. 1021–1027.

[5]Klunker, E. B., South, J. C., Jr., and Davis, R. M., "Calculation of Nonlinear Conical Flows by the Method of Lines," NASA TR R-374, Oct. 1971.

Counter-Rotating Structures over a Delta Wing

J. P. Hubner* and N. M. Komerath†
Georgia Institute of Technology, Atlanta, Georgia 30332-0150

Nomenclature

b	= wing span
b'	= local wing span
c	= root chord
$G()$	= nondimensionalized autospectral intensity function
L	= characteristic length
n	= Strouhal-scaled frequency, fL/U_∞
Re	= Reynolds number
t	= time
U_∞	= freestream speed
u, v, w	= streamwise, lateral, and vertical velocity, body coordinate system
x, y, z	= body coordinate system, origin fixed to model apex
α	= angle of attack
ϕ	= phase of trigger cycle

Superscripts

-	= time-averaged component of u, v, and w
^	= fundamental periodic component of u, v, and w
'	= random fluctuating component of u, v, and w

Introduction

THIS Note describes the experimental finding of counter-rotating structures, with axes oriented approximately spanwise, located between the surface and the vortex core on a 60-deg delta wing at high incidence. The finding is explained using laser sheet flow visualization and spectral analysis of hot-film data on and above the surface. It is confirmed by quantitative analysis of velocity data, synchronized in phase to the signal from a hot film. The finding is related to previous work on the origin and effects of such fluctuations, and its implications explored. A mechanism based on centrifugal instability is proposed.

Previous work at this and other laboratories[1–5] has shown that the vortex flowfield over a swept wing at 25–35-deg angle of attack develops organized velocity fluctuations under steady freestream conditions. The fluctuations are concentrated within a narrow frequency band but can only be described as quasiperiodic, with the phase not repeating exactly from cycle to cycle. These have been observed on isolated delta wings as well as on wing bodies and full models of fighter configurations. Reference 2 showed that the fluctuations maintain a constant value of reduced frequency (or Strouhal number) at a given angle of attack, over a large range of Reynolds numbers. Data at 20-deg angle of attack near the vertical tail of an F-15 model, extrapolated from $\frac{1}{32}$ and $\frac{1}{7}$ scale model tests using this constant Strouhal number, were shown to match the measured fin vibration frequency on a full-scale F-15. Flowfield studies on moderately swept (<60 deg) wings at angles of attack above 25 deg show that vortex breakdown occurs essentially at the apex. Reference 5 showed that the fluctuations originate close to the wing surface on a 60-deg cropped delta wing at or upstream of the 30% root chord station. They then amplify and focus into a narrow frequency band. The peak frequency decreases as the measurement location is moved downstream. In a crossflow plane at the wing trailing edge, the frequency content is uniform except in the postburst core region, where other phenomena appear to dominate. This Note focuses on the phenomena occurring near the surface. Redionitis et al.[6] attributed the fluctuations to vortex shedding; however, the velocity field over a 60-deg wing at $\alpha < 30$ deg is steady in the mean, and vortex shedding is not a plausible explanation. Gursul[7] proposed a helical mode oscillation in the postburst flowfield characteristic of moderately swept wings. The correlation with experimental evidence for sweep angles >60 deg was encouraging, but the correlation for sweep ≤60 deg was ambiguous. Although the geometry of the flow and the two-point surface pressure correlations of Gursul[7] do allow a helical mode description, this does not complete the physical explanation for the origin, amplification, and focusing of the phenomenon. Here we report on a detailed investigation using multiple planar, surface, and single-point measurement techniques. Spectral content of the fluctuations is measured using both hot films and laser velocimetry (LV). The velocity components are resolved using LV, thereby avoiding the ambiguity inherent in hot-film measurements.

Figure 1 shows the focusing and amplifying of the fluctuation energy for the 59.3-deg delta wing model.[4] The flow unsteadiness is visualized near the surface and under the core using laser sheets illuminated by smoke introduced through various surface ports, aligned parallel and perpendicular to the surface. Surface hot-film sensors and sensors in the flow above the wing are used to generate the spectra of the velocity fluctuations and to determine the frequency

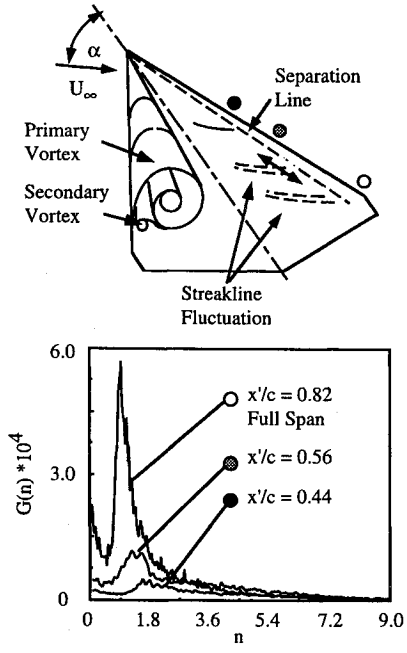

Fig. 1 Autospectra of velocity fluctuations along the leading edge of a 59.3-deg delta wing, measured using a single hot-film sensor oriented spanwise.

Received July 6, 1995; revision received Jan. 9, 1996; accepted for publication Feb. 9, 1996.

*Graduate Research Assistant, School of Aerospace Engineering. Student Member AIAA.

†Professor, School of Aerospace Engineering. Associate Fellow AIAA.

Table 1 Test matrix

Test type	U_∞, m/s	$Re_c \times 10^{-6}$	α, deg
Flow videography	1.52	0.04	15, 18, 20, 25, 30
Flow videography	6.10	0.16	20, 25
Hot-film anemometry	1.52, 6.10, 12.2	0.04, 0.16, 0.32	18, 25
Phase-resolved LV	6.10	0.16	25

of the spectral peak. The repetition rate of patterns in the laser sheet images is counted from video frames and checked against the hot-film spectra peak, both by extrapolation to higher velocities and by direct measurement. The structures are then captured quantitatively by laser velocimetry—phase synchronized with a trigger generated from a surface hot-film sensor at the upstream end of the measurement grid.

Experimental Procedure

The flat-plate cropped delta wing model with 18-deg windward beveled edges has a leading-edge sweep of 59.3 deg and a taper ratio of 0.062 (Ref. 4). The root chord and span are 398 and 386 mm, respectively. Surface flow videography and LV tests were conducted in a 1.07 × 1.07-m open circuit, low-speed wind tunnel. A 6-W argon-ion laser provided the sheet illuminating the streaklines that were created by entraining theatrical fog at very low pressure from 10 ports (1.4 mm in diameter) along the leeward surface of the delta wing, inboard of the secondary separation line. The video recording was mixed with a frame code to enable a field resolution of $\frac{1}{60}$ s. The region of surface illumination ranged from the surface to 3 mm above the surface.

The streamwise and vertical components of the velocity were measured separately. An external trigger signal was generated from the signal of a hot-film anemometer sensor mounted on the surface at the upstream end of the LV measurement grid. The LV data were resolved into 30 bins over the period of the dominant frequency measured using the hot film, thus giving a phase resolution ϕ of 12 deg. A total of 40,000 points were taken at each location. The mean and rms deviation of the value in each bin were computed. The synchronization of the LV measurements allowed the instantaneous streamwise and vertical velocities at any point to be decomposed, without loss of generality, into the time-averaged, the periodic fluctuation, and the random fluctuation velocities as in Eq. (1), respectively:

$$u(t) = \bar{u} + \hat{u}(t) + u'(t), \qquad w(t) = \bar{w} + \hat{w}(t) + w'(t) \quad (1)$$

The matrix of test conditions for both the flow videography and LV is shown in Table 1. Details of the hot-film anemometry are discussed in Ref. 5.

Results and Discussion

Surface flow videography showed the development of streakline fluctuations inboard of the secondary separation line. Figure 2a compares successive images of the surface streaklines. The two upstream smoke traces appear relatively smooth; however, streaklines closer to the trailing edge show kinks and relative displacements that correspond to their fluctuation. The origin of the fluctuations moved upstream with increasing angle of attack. Fluctuating streaklines from successive ports were not in phase and gave the impression of a slower convective movement downstream. Table 2 lists the port location of initial fluctuation vs angle of attack for $U_\infty = 1.52$ m/s. Similar results were obtained for higher U_∞.

At $\alpha = 25$ deg, the frequency of the observed waving of the streaklines was measured from the video and compared with off-surface hot-film sensor results acquired above the port at the same and higher freestream speeds. The frequency of the spectral peak, when scaled by the local semispan and freestream speed, compares well with scaled frequencies determined from the video: 0.89 and 0.91, respectively, for $b'/b = 0.5$–0.61 and 0.65 for $b'/b = 0.8$.

Lateral cross-sectional views of the streaklines displayed fluctuations of the secondary separation line as well; however, seeding was too irregular for frequency determination. Streamwise views,

Table 2 Port location of fluctuating streakline origin

α, deg	15	18	20	25	30
b'/b	1.0	0.8	0.6	0.4	<0.2

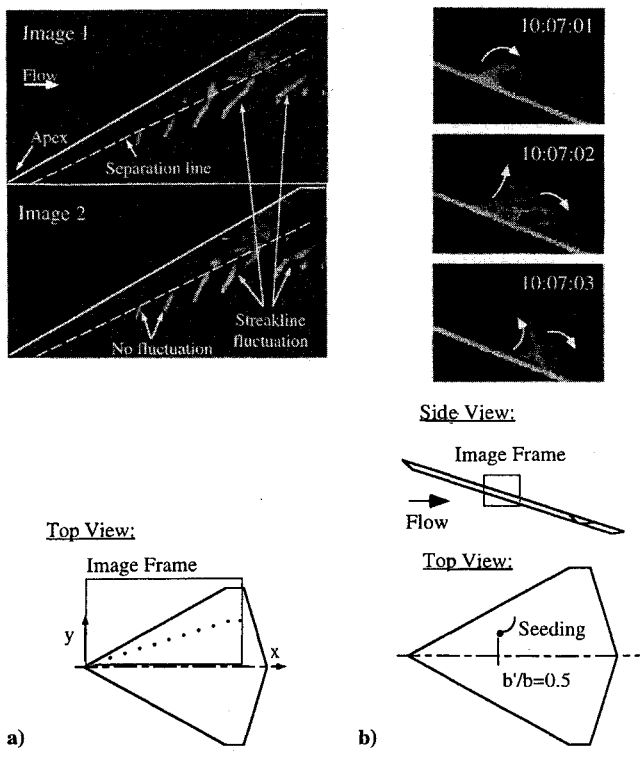

Fig. 2 a) Streaklines of smoke emanating from several surface ports, seen in a 1-mm-thick laser sheet oriented parallel to the surface of the 59.3-deg delta wing, at α = 20 deg and U_∞ = 1.51 m/s and b) counter-rotating roll-up of the smoke in a laser sheet oriented perpendicular to the wing surface and along a ray inboard of the secondary separation line, at α = 25 deg and U_∞ = 1.51 m/s.

Fig. 2b, showed streakline roll-up and eruption (off the surface) inboard of the secondary separation line, giving the appearance of a three-dimensional vortical structure. The amplitude of the waving motion and the size of the structures were larger for streaklines exiting the downstream ports. The sense of the rotation appeared to be the same but was not clear from the videography alone.

Frequency domain comparisons between the LV and a surface hot-film signal (external trigger source) showed that the LV signal was able to resolve the frequency content within the flow. Data rates of 10–40 times the peak fluctuation were obtained, thus avoiding errors because of the digital-to-analog step-like signal. The phase-resolved velocity data displayed a periodic variation in velocity over most of the trigger cycle. Over the latter 20% of the trigger cycle, however, the number of data points acquired per bin decreased as a result of the drifting of the fundamental frequency. This is quasiperiodicity: while the dominant frequency content is constant, cycle-to-cycle repeatability is absent. This deviation from periodicity causes severe attentuation, by a factor of 5 compared with the spectral peak, during the ensemble averaging.

Figure 3 shows the measurement plane and the phase-resolved fluctuating velocity vectors for at $\alpha = 25$ deg. Because the bandwidth of the fluctuations increases near the (postburst) core trajectory, and the peak frequency increases further upstream, the region of validity of a given trigger signal is limited in size. This limited the extent of the LV measurement grid. The total fluctuating streamwise and vertical velocities in Fig. 3 are nondimensionalized by U_∞. Six different phases of the fluctuation cycle are shown for the plane at $2y/b = 0.5$. Instantaneous streamlines interpolated from the vectors help clarify the structures. With respect to a spatial frame fixed in time, the fluctuations form lateral, counter-rotating structures with distinct regions of up and down flow. The

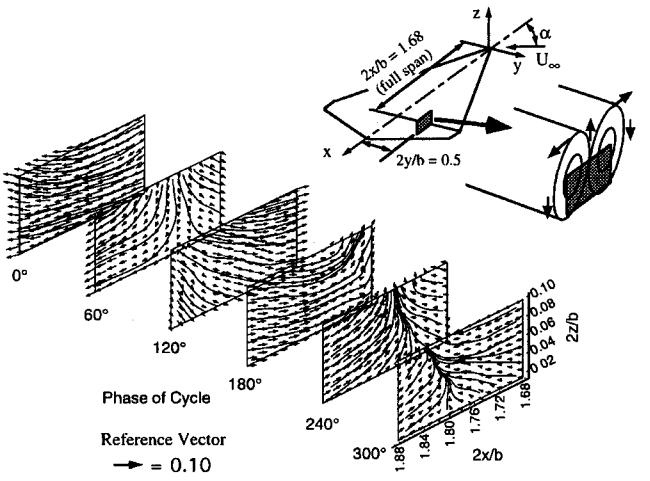

Fig. 3 Vectors of fluctuating velocity, measured using laser velocimetry, of ensemble-averaged in several discrete 12-deg phase intervals of a trigger signal at the dominant fluctuation frequency generated from a surface hot-film sensor at $2x/b = 1.68$.

structures convect downstream with respect to time (phase). Single-point measurements above the core were 180 deg out of phase with corresponding points below, suggesting a helical geometry of propagation of the disturbance. The structure scale is on the order of the vortex radius; the convection speed based on this length scale and the cycle period is $0.15U_\infty$.

The formation of a rotating structure in an environment with mean streamline curvature is analogous to Taylor–Görtler type vortices[8,9] and indicates the interaction between the centrifugal forces and the radial pressure gradient of the primary vortex near the surface. This type of instability is based on Rayleigh's second theorem on the stability of a velocity profile; the conditions exist in the surface shear layer under a postburst vortex, whose tangential velocity profile resembles that of solid-body rotation. Ludwieg[10] proposed that this type of three-dimensional disturbance causes the breakdown of free vortices over delta wings. Disturbances of this nature could explain the focusing and amplification mechanisms away from the core.

Some similarities are observed with Gursul's helical mode explanation.[7] The trajectory of the structures does appear to be helical, as may be expected given the mean streamlines of the vortex flow. In addition, the spectral frequency remains approximately constant over a crossflow plane at a given chordwise location. However, several features do not fit the helical mode theory. The orientation of the structures, with velocity components measured unambiguously, is essentially spanwise, not chordwise as postulated by Gursul based on hot-film data. The phenomenon clearly does not originate in the core region, postburst or otherwise. It originates in the shear layer near the surface.

Conclusions

Velocity fluctuations occurring in the postburst flowfield over a 59.3-deg delta wing were studied using laser sheet videography, hot-film anemometry, and LV.

1) Viewed in a plane parallel to the wing surface, surface layer streaklines oscillated at a frequency that matched that of the spectral peak measured using hot-film anemometry.

2) Viewed in a vertical plane along a ray inboard of the secondary separation line, the streaklines rolled up and erupted off the surface, indicating counter-rotating structures.

3) Spectra measured using LV above the surface matched those measured by a surface hot film.

4) Velocity measurements, triggered from the surface hot-film signal, resolved into the phase of the spectral peak frequency and ensemble averaged, showed organized, counter-rotating structures in two vertical planes aligned with rays. These clearly indicate vortical structures whose axes are oriented approximately spanwise, convecting at a speed of roughly $0.15U_\infty$.

5) The nature of the structure appears consistent with a centrifugal instability arising between the primary vortex and the surface.

Acknowledgments

This work was performed under a U.S. Air Force Office of Scientific Research grant monitored by Dan Fant and Len Sakell. Special thanks are given to the Experimental Aerodynamics Group for its assistance.

References

[1]Colvin, B. J., Mullans, R. E., Paul, R. J., and Roos, H. N., "F-15 Vertical Tail Vibration Investigations," McDonnell–Douglas Corp., Rept. A6114, St. Louis, MO, Sept. 1979.

[2]Komerath, N. M., Schwartz, R. J., and Kim, J. M., "Flow over a Twin-Tailed Aircraft at Angle-of-Attack, Part II: Temporal Characteristics," *Journal of Aircraft*, Vol. 29, No. 4, 1992, pp. 553–558.

[3]Klein, M. A., Hubner, J. P., and Komerath, N. M., "Spectral Measurements in Vortex Flow over Swept-Winged Configurations at High Angle of Attack," AIAA Paper 94-1804, June 1994.

[4]Hubner, J. P., and Komerath, N. M., "Trajectory Mapping of Quasi-Periodic Structures in a Vortex Flow," *Journal of Aircraft*, Vol. 32, No. 3, 1995, pp. 493–500.

[5]Hubner, J. P., and Komerath, N. M., "Visualization of Quasiperiodic Structures in a Vortex Flow," AIAA Paper 94-0624, Jan. 1994.

[6]Redionitis, O. K., Stapountzis, H., and Telionis, D. P., "Vortex Shedding over Delta Wings," *AIAA Journal*, Vol. 28, No. 5, 1990, pp. 944–946.

[7]Gursul, I., "Unsteady Flow Phenomena over Delta Wings at High Angle of Attack," *AIAA Journal*, Vol. 32, No. 2, 1994, pp. 225–231.

[8]Schlichting, H., *Boundary Layer Theory*, 7th ed., McGraw–Hill, New York, 1979, pp. 525–535.

[9]Saric, W., "Görtler Vortices," *Annual Review of Fluid Mechanics*, Vol. 26, 1994, pp. 379–409.

[10]Ludwieg, H., "An Explanation of the Instability of the Free Vortex Cores Occurring over Delta Wings with Raised Edges," NASA TM-75861, 1980; translated from *Zeitschrift für Flugwissenschaften*, Vol. 10, No. 6, 1962, pp. 242–249.

Three-Dimensional Analysis of Simply Supported Laminated Cylindrical Shells with Arbitrary Thickness

Jianping Zhou* and Bingen Yang†
University of Southern California, Los Angeles, California 90089-1453

Introduction

MODELING of composite cylindrical shells and panels is usually based on one of the following three types of theories: the classic laminated theory (CLT), the shear deformation theories, and the three-dimensional elasticity theory. Because of the high ratio of in-plane Young's modulus to transverse shear modulus, ignorance of the shell transverse shear deformation in CLT can lead to serious errors even for thin cylindrical shells/panels. Although the shear deformation theories have met with success in many cases, three-dimensional elasticity solutions are still needed for the purpose of assessment of various approximate theories and better understanding of actual distributions of stresses, strains, and displacements in composite shells, especially for thick shells.[1,3,4,6,7] This Note presents an innovative method for analysis of simply supported (SS), multilayered, orthotropic, circular cylindrical shells and panels with arbitrary shell thickness. In this method, the three-dimensional displacements and stresses of laminated shells are determined by a

Received Sept. 13, 1994; revision received Oct. 13, 1995; accepted for publication Nov. 1, 1995.

*Visiting Scholar, Department of Mechanical Engineering; currently Professor, Department of Astronautics, National University of Defence Technology, Changsha, Hunan 410073, People's Republic of China.

†Associate Professor, Department of Mechanical Engineering. Member AIAA.